Open Access
Full Length Article

ORIGINAL ARTICLE

Comparison of Neural Networks and Support Vector Machines for the Mass Balance Ablation Observation of Glaciers in Baltoro Region

Nasru Minallah[1], Waleed Khan[2]

[1, 2] Department of Computer Systems Engineering, University of Engineering and Technology, Peshawar, KPK, Pakistan

ABSTRACT

Glaciers are melting rapidly across poles due to climate changes. Apart from poles, land-based glaciers are also melting dramatically. It is crucial to monitor and reduce the rapid melting of glaciers. However, on-site monitoring of glaciers is challenging, costly, time-consuming, and entails subjectivity. Therefore, remote sensing techniques are indispensable to provide an automated and cost-effective solution in order to enhance the land-based monitoring of glaciers. This work presents a remote sensing technique that is based on neural networks (NN) and support vector machines (SVM) used for monitoring Baltoro glaciers, situated in the Karakurum range. The classifier classifies land, cloud, greenery, and the glacier mass. The data set used is the Landsat imagery from 1976, 1991, 1994, 2000, 2010, 2013 and 2016 including June and July. We observe that SVM achieves an accuracy of 99.97 %, while ANN attains an accuracy of 98.87 %. The results show that the glaciers have experienced a significant ablation in their masses with the temperature rise around the globe.

Keywords: Feed Forward Neural Networks, Glacier mass balance, Support Vector Machines, Geographical Information System, Landsat.

Author`s Contribution
[1,2]Manuscript writing, Data Collection Data analysis, interpretation, Conception, synthesis, planning of research, and discussion

Address of Correspondence
Waleed Khan
Khanwaleed247@uetpeshawar.edu.pk

Article info.
Received: Dec 21, 2017
Accepted: Oct 07, 2018
Published: Dec 30, 2018

Cite this article: *Minallah N, Khan W. Comparison of Neural Networks and Support Vector Machines for the Mass Balance Ablation Observation of Glaciers in Baltoro Region. J. Inf. commun. technol. robot. appl.2018; 9(2):37-45.*

Funding Source: *NCBC, UET Peshawar & HEC Islamabad*
Conflict of Interest: *Nil*

INTRODUCTION

Around the globe, glacier melting has been one of the biggest problems that humanity is facing for the last few decades. Due to this phenomenon, we are experiencing a rise in temperatures across the globe. Recent studies reveal, that due to the melting of permafrost owing to rising temperatures and glacier melting, the earth is going towards an excess release of carbon gases in the atmosphere [1] [2]. The melting glaciers and their impact on the global atmosphere have compelled Engineers, Scientists and Environmentalists to focus on proposing new methods for reducing carbon emission that is destroying the Ozone Layer [3]. In order to preserve this resource, new techniques must be researched for better classification of Glaciers using remote sensing. For this purpose, we compared two stat of the art classifiers in this work i.e. FFNN and SVM. A comparison of the mentioned classifiers has been provided in this work, since FFNN and SVM have proven

to be state of art classifiers in various applications, including glaciers classification. SVM is a kind of classifier that takes the training data and visualizes a hyperplane among different classes. SVM is also considered a discriminate classifier. While on the other hand FFNN is based on Artificial Neural Networks (ANN) which has been derived from the biological neural networks that constitute the animal brain. Comparison of these classifiers has been done with respect to their accuracy wiz. A number of correct predictions from all predictions made by the classifier based on our ground truth data. This method helps in finding the quality metric of the classifier. The greater the accuracy, the better the results of the testing data. The region selected for our experimentation is Baltoro Glacier. Baltoro is the world's largest land-based glacier due to its immense length and area in the Karakorum Range.

- This work compares two state-of-the-art classifiers i.e., FFNN and SVM for detecting glacier ablation.
- Furthermore, we explore the best classifier for classifying the glacier mass.

We provide a remote-sensing-based and a cost-effective solution for measuring the decline in Baltoro glacier mass balance and its surrounding glaciers. The rest of the paper is organized as follows. Section 2 discusses related work. The retrieved data is discussed in Data Description i.e., section 3 while section 4 is about Methodology. Section 5 discusses the experimental results. Furthermore, the Conclusion of the work is explained in section 6.

LITERATURE REVIEW

Remote sensing can acquire regional information about glaciers instantly and has proven as a significant tool to monitor and study the changes occurring in glaciers [4]. Himalaya and Karakorum mountains comprise of 17%and 37% as glacier ice, respectively [5]. Glaciers cover about 30% of the earth's land surface in which 10% is permanently ice-covered at present, and 10% is permanently frozen. The land in the northern hemisphere is 50% covered by snow and ice in a winter season. Glaciers are the source of more than 75% of the world's fresh water through which we irrigate lands of densely populated areas. The analysis has been done in regards to volume, high altitude thickness, and area of the glacier [6]. Neal R. Iverson et al. performed an analysis of the effects of basal debris on the flow of glaciers [7]. DEMs were used to find about the volumetric changes that occurred in the glacier.

Different techniques and procedures are presented by D.Lu to perform change detection using remote sensing [8]. ANN, Spectral Mixture Analysis, and integration of remote sensing data and GIS turned out to be important methods for change detection applications. Every method has its own significance depending on its application [8]. In [9] analysis on snow, cover distribution was done in Aksu Catchment (Central Tien Shan) using level 1b scenes of AVHRR. To show widespread glacier wastage in the central, eastern and southwestern parts of the Hindu Kush–Karakoram–Himalaya region during 2003–08. In [10] an extensive analysis has been done on change detection methods using optical remote sensing. Each technique has been explained in detail.

2.1. Remote Sensing Based Techniques

Glaciers can be detected using classification algorithms having different accuracy rates. For instance, supervised and object-based classification is relatively more effective than knowledge-based in order to detect glaciers change with an accuracy of 95%, 93%, and 86%, respectively [8]. P.Rastner et. al discusses two techniques for Glacier classification i.e. Pixel-Based and Object-Based for Optical Satellite Images [11]. V.Akbari et al. in [12] propose a system for the detection of changes in Arctic glaciers using multi-temporal and multi-polarization synthetic aperture radar (SAR) images. In [13] robust image ratio method for exploiting the dense temporal image coverage of sentinel and Landsat 8 is proposed. In [14] E. Erten et al. monitor the glacier velocity by Maximum Likelihood Texture Tracking system. In order to promote decision making, the understanding of relationship and interaction between human and natural phenomenon, the timely and accurate detection of earth surface features are important and indispensable [8]. Momentous amount of work is done on polar ice caps as well. [15] has used satellite laser altimetry and a global elevation model. Furthermore, time series from 1986-2013 was generated using level 1b scenes of AVHIR and Moderate Resolution Imaging Spectrometer data, that were classified using a dichotomous decision scheme and MODIS data [9]. A sensor system developed by

Rodriguez Moralas et al. operates over different frequency bands ranging from 160 MHz-18 GHz. Rodriguez Moralas et al. mounted the sensor on aircraft providing extensive support for observing terrain in Polar Regions that could be impossible for scientists to visit and observe directly. The operation of these sensors is based on different bands that range from 16 MHz-18GHz [16]. Similarly, Callegari et al. performed a supervised classification of ice, soil, and snow using SVM. To obtain images of Eastern Italian Alps through aerial photography Synthetic Aperture Radar (SAR) and Polarimetry (POL-SAR) was used [17]. Furthermore Ke et al. used multi-source and multi-temporal data acquired from ICESat and Landsat to evaluate the changes occurred in Qinghai-Tibet plateau [18]. Zhang et al. determine continental area change of glaciers and their melted lakes located in the northern margins of Qinghai- Tibet Plateau using Landsat TM/ETM+ images from 1991 to 2009 [4]. P.Peduzzi et al. evaluate the occurred changes in Nevado Coropuna (Peru) using GIS and Remote Sensing [6].

On monitoring glacier changes, a large number of Glaciological Studies are focusing on using remote sensing in regions that are experiencing rapid changes in glaciers located in Alaska [19]. Haeberliv W. et al. Discusses Extensive details about Glacier Mass Balance. The sum of all processes that add mass to a glacier and remove mass from it is called the mass balance of a glacier. Addition of mass to a glacier commonly takes place in the form of snowfall. The predominant form of ablation is the melting of snow and ice in summers [20].

DATA DESCRIPTION

Analysis has been conducted on Landsat Imagery, acquired from the USGS official website [21] for the month of June and July to ensure the same temporal resolution of the dataset. The first Landsat satellite was launched on 12 July 1972 for earth exploration via remote sensing. Currently, Landsat 8 is the functional satellite providing its services in retrieving images and transmitting them back to the observatory.

Due to the non-availability of Landsat data from 1980-1989, the retrieval of data from the mentioned years was not possible. Level 1 imageries of Landsat2, Landsat3, Landsat5, Landsat7, and Landsat8 have been retrieved, which include multispectral images of the desired scenes with Landsat 2 having a spatial resolution of 60m while the rest of the data having a spatial resolution of 30m. The spatial resolution of the panchromatic band is 15m, but only Landsat 7 and Landsat 8 have panchromatic sensors installed into the satellites as an additional band 8. Data with a cloud cover of less than 20% have been retrieved to ensure noise free information.

3.1. Shape Files

While the shapefiles of the focused region have been acquired from the GLIMs and open street map [22] through their online resources. The international program GLIMS monitors the extent, changes, and dynamics of glaciers worldwide using satellite data [23]. GLIMS is a project designed to monitor the world's glaciers primarily using data from optical satellite instruments, such as ASTER(Advanced Spaceborne Thermal Emission and Reflection Radiometer). According to reports of NASA of July 2016 was recorded to be hottest in the history of mankind. First, six months of 2016 were warmest in NASA's modern temperature records, which dates back to 1880 [24].

RESEARCH METHODOLGY

The Methodology section entails Pre-Processing, Region-Extraction, Feature-Extraction, and Classification. Furthermore, the classification section further leads to FFNN and SVM. Algorithm 1 represents the performed steps for the completion of this work.

4.1. Pre-Processing

Images obtained needed to be processed in order to make them usable for further processing. This includes image sharpening, enhancement, and contrast stretching to see dark objects adjust the angle of our need and select the proper coordinate system also called registration for further processing [26]. After thoroughly analyzing the satellite data we concluded that extraction of our Baltoro Glacier region from satellite data is necessary to enhance and objectify our results. Furthermore, the processing time for the classifier will also be decreased. For such purpose, GLIMS provided us with the shapefiles for Baltoro Glacier as discussed above. As shown in figure 1, after applying shapefile we can easily locate Baltoro Glacier boundary by pointing out the red polygon.

```
Algorithm 1 Experimental Setup Algorithm
Data Acquire ();
for i ← Alll mages do
        Image Acquisition ();
           Image Enhancement ();
           Contrast Stretching ();
 // Extraction of Baltoro Region from Landsat Scene
          Region Extraction ();
 // Feature Extraction of the training data for classifiers
          Feature Extraction ();
      end
      for j ← Extracted Region do
         for k ← Extracted Features do
           if FFNN  then
             Set Parameters ();
               Classification ();
               10 Epochs ();
               100 Epochs ();
               1000 Epochs ();
       // Accuracy Assessment of Classifiers
           Accuracy Assessment ();
           end
           if SVM then
           Set Parameters ();
              Classification ();
              Linear Kernal ();
              2 Degree Polynomial Kernal ();
              Radial Basis Kernal ();
              Sigmoid Kernal ();
       // Accuracy Assessment of Classifier
           Accuracy Assessment ();
            end
         end
      end
      Accuracy Comparison ();
```

4.2. Future Extraction

After pre-processing and clipping phase, feature extraction has been performed in order to obtain ground truth data for training classifiers. Features have been extracted using ROI (Region of Interest). Different polygons for land, ice, debris, and clouds have been selected. These polygons have been selected in the desired regions manually as training data.

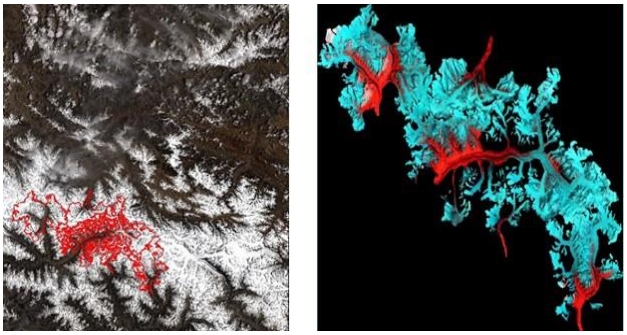

Figure 1 Region of Interest chosen for experimentation

4.3. Classification

A comprehensive comparison of Feed Forward Neural Networks and SVM has been performed, to find a classifier which produces best classification results.

Feed Forward Neural Networks

FFNN consists of a substantial number of units called nodes, organized in layers, through connections comprising of different weights. Data enters the input layer and passes through the network and arrives into the output layer. There is no feedback or loops in FFNN that is why it is called Feed Forward Neural Network as illustrated in figure 2.

A two-layered network is presented in figure 2. 5 output units at the top layer, represented in red. Blue is the hidden layer, shown in the middle layer. The bottom units are represented as inputs that comprise three in number. Between the two layers in figure 4 are connections having different weights. These weights are subjugated according to the fittest data.

$$\int_{i=0}^{n} = w_i x_i$$

The weights are represented as w i to the input xi. The Activation function is as under:

$$f(x) = \frac{1}{1+e^{x}}$$

Here the excitation level of input data is represented by 'x' i.e. neurons.

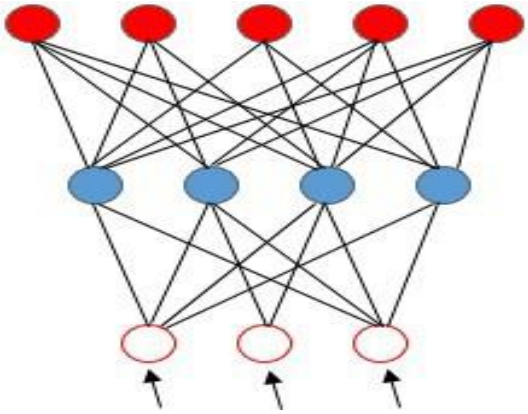

Figure 2 Feed Forward Neural Networks basic model

Input data has been provided to the network during the learning phase of the classifier. The training threshold determines the size of the internal weight for the activation of the node. Weights are adjusted between the nodes for better classification results in order to minimize error during the training phase. It must also be considered that poor generalization may be caused by too many weights. Likewise, the speed of the training phase determines the training Rate. Non-convergence may be imminent with a large training phase. The results using FFNN are obtained using algorithm 2.

```
Algorithm 2 Feed Forward Neural Networks
// Setting the Threshold value of Classifier
Set Threshold value ();
// To set the training Rate of the classifier
Set Train Rate ();
Set Training momentum ();
// To set the root mean square error of Classifier
Set RMS Criteria
// Set Number of Hidden Layers of Neural Networks
Classifier
Set Hidden Layers;
// Train  certain number of Epochs Neural Networks
Classifier
for i do
if the error is acceptable then
Stop, and exit the loop
end
Increment the hidden layer by one
Apply the weight of the new hidden unit
end
```

Support Vector Machines

SVM was first introduced by Bose, Guyon, and Vapnik [27] as a state of art classification method. SVM is also used in pattern Recognition and Regression estimation. The main reason for the wide usage of SVM classifiers is its high computational efficiency. A decision boundary also called hyper line is estimated in such a way that pixels belonging to different classes can be differentiated easily. The hyper line depends on the kernel used during the training of classifier using training data i.e. ground truth. Different types of kernels include Linear, Polynomial, Sigmoid and Radial. In our case study Linear, Polynomial, Sigmoid and Radial Based kernel has been used.

Linear: $K(x_i, x_j) = x_i^T x_j$

Polynomial: $K(x_i, x_j) = (g\, x_i^T x_j + r)^d,\ g > 0$

Sigmoid: $K(x_i, x_j) = \tanh(g\, x_i^T x_j + r)$

Radial basis function (RBF): $K(x_i, x_j) = e^{(-g(x_i - x_j)^2)}$

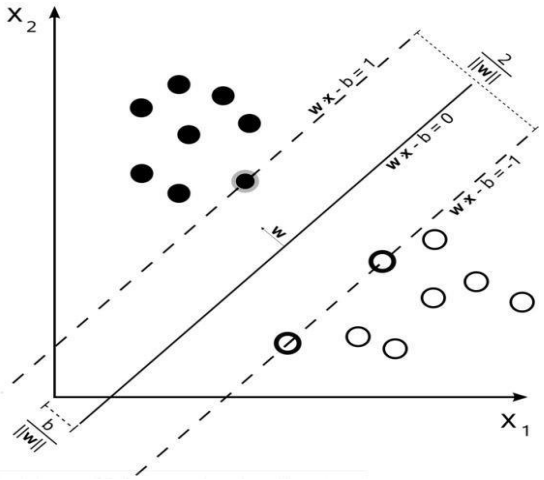

Figure 3 As shown in the figure, there are multiple hyper plane (dashed lines) in the graph shown by

Where d determines the degree of the polynomial kernel used. The degree may be 2, 3 and so on. Degree of the polynomial determines the delineation factor of the hyperplane between the classes. A Polynomial with degree 1 represents a linear kernel. The high degree may increase the variability of classifier but may also introduce noisy data. In case of Linear Kernel, a straight line is used to separate those features of problem space during the training of the classifier. Let's suppose a training data set of a finite number of points is given, as:

$(x_1, y_1) \ldots\ldots\ldots\ldots (x_n, y_n)$

Where the y i is the class name and x i is the feature set for the designated class. Class may be either 1 or -1. To determine an offset value using which a boundary may be defined, a hyperplane must be estimated as shown in figure 3 in order to designate the unknown feature either to class 1 or -1 during the testing phase of the data. The hyperplane may be defined as:

$$\vec{w} \cdot \vec{x} - B = 0$$

Where w is hyper plane's normal vector.

The Algorithm for SVM is listed in Algorithm 3.

```
Algorithm 3 Algorithm for Support Vector Machines
Set Kernel Type ();
Set Penalty Parameter ();
for i ← Get Image do
  if Penalty does not apply then
    if Kernel = Linear then
      Classification ();
end
if Kernel = Polynomial then
  Set Degrees ();
   // For the separation of margins of hyper plane
from origin
   Set bias ();
  // For the control of variance of the data
    Set Gamma (); Classification ();
end
if Kernel = Sigmoid then
    // For the separation of margins of hyper plane
from origin
    Set bias ();
   // For the control of variance of the data
    Set Gamma (); Classification ();
end
if Kernel = RBF then
    // For the separation of margins of hyper plane
from origin
   Set bias;
    // For the control of variance of the data
    Set Gamma (); Classification ();
end
end
Exit ();
end
```

EXPERIMENTAL RESULTS

5.1. Hardware/Software

We ran our experiments on an Intel i5-6500 core machine with a total of 4 cores and each core is clocked at a frequency of 3.2 GHz. The machine supported 39 bit physical and 48-bit virtual addresses. Multiple Instruction

Per second (MIPS) was 6384. The machine had a memory of 8 GB sufficient enough to support the processing, classification, and analysis of the glacier data. The machine had storage of 1 TB. The operating system used was Professional Windows 10.

5.2. Impact of FFNN

Shown in figure 4 is the Root Mean Square error (RMS) Plot that determines to stop further classification after a certain threshold is reached. Figure 4 shows the RMS error graph vs iterations graph. Although the graph shows the analysis of 1000 iterations it can be realized from the graph that the classifier was put to stop at 300 iterations. This happened because RMS value equaled 0.10 which was the predefined value for the classifier.

1 hidden layer has been set for FFNN classifier. Different weights are assigned to each connection, when data representing a selected feature class, reaches the output layer after passing through the hidden layer. The predicted 10 training data which is weighted more than that is predicted incorrectly.

Results generated by experimenting on FFNN has been obtained by setting the following parameter values for the classifier, which are presented in t.

- Training Threshold = 0.9
- Training Rate =0.2
- Number of Hidden Layers =1
- Training RMS exit criteria
- Training Momentum = 0.9

5.3. Impact of SVM

Since our feature sets have mostly been pixels so we used only polynomial degree 2 kernel in our experimentation. t is the bias in the polynomial and RBF kernels. The term bias in the SVM is very important because without it the hyperplane will always pass through the origin and hence our classifier may not provide good accuracy results. In our experimentation 1 has been used as a bias parameter for the SVM classifier.

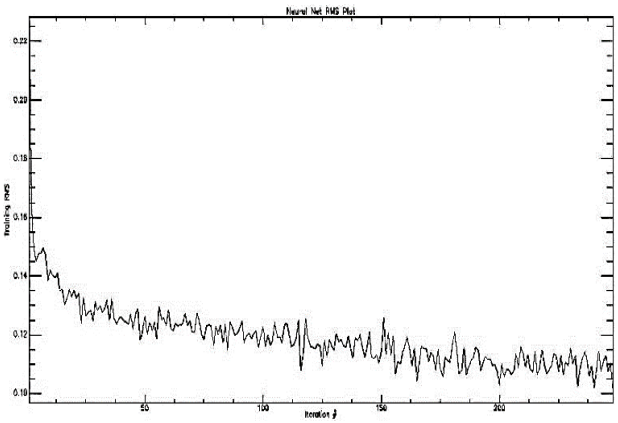

Figure 4 Training RMS exit criteria

Table 1. The Table shows the Comparison of accuracy assessment tests conducted on testing data on classification images. Column one shows the quantity of data to be tested while column 2, 3 and 4 represent its accuracy on 10, 100 and 1000 iteration of Neural Network classifier respectively. Similarly, for SVM classifier the accuracy for linear, polynomial degree 2, radial basis function, and sigmoid has been calculated via testing 10 percent, 30 percent, 50 percent, 80 percent and 90 percent of testing data.

Classifier Accuracy							
Feed Forward Neural Networks				SVM			
Epochs				Kernel			
Training Data	*10*	*100*	*1000*	Linear	2-degree Polynomial	RBF	Sigmoid
10%	97.92%	97.35%	97.96%	98.65%	98.73%	98.89	95.47%
30%	96.57%	97.29%	97.94%	98.81%	98.90%	98.99	95.20%
50%	96.68%	97.30%	97.93%	98.82%	98.91%	99.01	95.30%
80%	96.71%	97.27%	97.95%	98.86%	98.94%	99.02	95.30%
90%	96.73%	97.38%	98.00%	98.87%	99.97%	99.04	95.33%

5.4. Impact of SVM

Table 1, shows the results generated by training and testing the two classifiers for comparison purposes. Testing data in the table represents the percentage of data provided to the classifier for training purposes and the following columns show the accuracy results of FFNN and SVM classifiers.

Different percentages of the collected data have been taken, i.e. 10%, 30%, 50%, 80%, and 90%. In 'Feed Forward Neural Networks' column 10, 100 and 1000 epochs have been taken and their results have been mentioned in their respective columns.

It can be observed that as the epochs increase from 10 to 100 the accuracy of classifier shows different results while for 1000 epochs as the training data increases so does the accuracy of the classifier. In the section of 'SVM', linear, 2-degree polynomial, Radial Basis Function and Sigmoid have been mentioned and their respective results have been included in their respective columns. Similarly, it can be analyzed that as the training data increases from 10% to 90% the accuracy also increases. i.e. for 90% the classifier accuracies calculated for the parameter of linear, 2-degree polynomial, Radial Basis Function, and Sigmoid are 98.86%, 98.99%, 99.04%, and 95.33%. As compared to 10%, 30%, 50%, 80%, the results gathered from using 90 % of training data shows better results.

CONCLUSION

SVM using RBF (Radial Basis Function) having an accuracy of 99.04% has proved to be a comprehensive classifier for glacier and land data as compared to Neural Networks with the accuracy of 98.00%, in our experiments. The experiments have been conducted of a vast number of Landsat images ranging from 1979 to 2016. SVM classifier due to its kernel based nature has proved to be a better choice for classification of glaciers. Change detection and mass balance ablation in glaciers can be substantially done using volumetric studies of the area. This type of studies not only show us the altitude and amplitude of the glacier mass, but also the displacement of glacier masses due to temperature changes in the region, which involves our future study.

REFERENCES

1. Fort M. Permafrost in the Himalayas: specific characteristics, evolution vs. climate change and impacts on potential natural hazards. In: EGU General Assembly Conference Abstracts. vol. 17 of EGU General Assembly Conference Abstracts; 2015. p. 4733.
2. Schuur E, McGuire AD, Sch¨adel C, Grosse G, Harden J, Hayes D, et al. Climate change and the permafrost carbon feedback. Nature. 2015; 520(7546):171.
3. Marzeion B, Champollion N, Haeberli W, Langley K, Leclercq P, Paul F. Observation-based estimates of global glacier mass change and its contribution to sea-level change. In: Integrative Study of the Mean Sea Level and Its Components. Springer; 2017. p. 107–132.
4. Zhang L, Guo H, Ji P, Chen J. A research of glacier change in West Kunlun through remote sensing. In: Geoscience and Remote Sensing Symposium (IGARSS), 2012 IEEE International. Ieee; 2012. p. 4430–4433.
5. Williams MW. The Status of Glaciers in the Hindu Kush–Himalayan Region. Mountain Research and Development. 2013;33(1):114–115.
6. Peduzzi P, Herold C, Silverio Torres WC. Assessing high altitude glacier thickness, volume and area changes using field, GIS and remote sensing techniques: the case of Nevado Coropuna (Peru). Cryosphere. 2010; 4(3):313–323.
7. Iverson NR, Cohen D, Hooyer TS, Fischer UH, Jackson M, Moore PL, et al. Effects of basal debris on glacier flow. Science. 2003; 301(5629):81–84.
8. Lu D, Mausel P, Brondizio E, Moran E. Change detection techniques. International journal of remote sensing. 2004; 25(12):2365–2401.
9. Peters J, Bolch T, Gafurov A, Prechtel N. Snow cover distribution in the Aksu catchment (central Tien Shan) 1986–2013 based on AVHRR and MODIS data. IEEE Journal of Selected Topics in Applied Earth Observations and Remote Sensing. 2015; 8(11):5361–5375.
10. Iverson NR, Cohen D, Hooyer TS, Fischer UH, Jackson M, Moore PL, et al. Effects of basal debris on glacier flow. Science. 2003; 301(5629):81–84.
11. Rastner P, Bolch T, Notarnicola C, Paul F. A comparison of pixel-and object-based glacier classification with optical satellite images. IEEE Journal of Selected Topics in Applied Earth Observations and Remote Sensing. 2014; 7(3):853–862.
12. Akbari V, Doulgeris AP, Eltoft T. Monitoring Glacier Changes Using Multitemporal Multipolarization SAR Images.IEEE Transactions on Geoscience and Remote Sensing. 2014 June; 52(6):3729–3741.
13. Winsvold SH, K¨a¨ab A, Nuth C. Regional Glacier Mapping Using Optical Satellite Data Time Series. IEEE Journal of Selected Topics in Applied Earth Observations and Remote Sensing. 2016 Aug; 9(8):3698–3711.
14. Erten E, Reigber A, Hellwich O, Prats P. Glacier Velocity Monitoring by Maximum Likelihood Texture Tracking. IEEE Transactions on Geoscience and Remote Sensing. 2009 Feb; 47(2):394–405.
15. Ka¨a¨b A, Berthier E, Nuth C, Gardelle J, Arnaud Y. Contrasting patterns of early twenty-first-century glacier mass change in the Himalayas. Nature. 2012; 488(7412):495.
16. Rodriguez-Morales F, Gogineni S, Leuschen CJ, Paden JD, Li J, Lewis CC, et al. Advanced multifrequency radar instrumentation for polar research. IEEE Transactions on Geoscience and Remote Sensing. 2014; 52(5):2824–2842.
17. Callegari M, Carturan L, Marin C, Notarnicola C, Rastner P, Seppi R, et al. A Pol-SAR analysis for alpine glacier classification and snowline altitude retrieval. IEEE Journal of Selected Topics in Applied Earth Observations and Remote Sensing. 2016; 9(7):3106–3121.
18. Ke L, Ding X, Zhang L, Shum C, Hwang C, Luo Y. Remote sensing of glacier distribution and change over the Qinghai-Tibet Plateau. In: Earth Observation and Remote Sensing Applications (EORSA), 2016 4th International Workshop on. IEEE; 2016. p. 442–446.
19. Arendt AA, Echelmeyer KA, Harrison WD, Lingle CS, Valentine VB. Rapid wastage of Alaska glaciers and their contribution to rising sea level. Science. 2002; 297(5580):382–386.
20. Haeberli W. Glacier mass balance. In: Encyclopedia of Snow, Ice, and Glaciers. Springer; 2011. p. 399–408.
21. National Aeronautics and Space Administration, GISS;. Accessed: 2017-09-30. //https://www.giss.nasa.gov. openstreetmap;. Accessed: 2017-07-6. //http://www.openstreetmap.org.
22. Muhammad S, Gul C, Javed A, Muneer J, Waqar MM. Comparison of glacier change detection using pixel-based and object-based classification techniques. In: Geoscience and Remote Sensing Symposium (IGARSS), 2013 IEEE International. IEEE; 2013. p. 4118–4121.
23. 2016 Climate Trends Continue to Break Records; Accessed: 2016-07 25.//https://www.nasa.gov/feature/goddard/2016/climatetrendscontinuetobreakrecords/.
24. USGS (United States Geological Survey), 1972-2016.; Accessed: 2017-06-17. //https://earthexplorer.usgs.gov.
25. Nakai K, Hoshi Y, Taguchi A. Color image contrast enhancement method based on differential intensity/saturation gray-levels histograms. In: Intelligent Signal Processing and Communications Systems (ISPACS), 2013 International Symposium on. IEEE; 2013. p. 445–449.
26. Boser BE, Guyon IM, Vapnik VN. A training algorithm for optimal margin classifiers. In: Proceedings of the fifth annual workshop on Computational learning theory. ACM; 1992. p. 144–152.
27. Minora U, Senese A, Bocchiola D, Soncini A, D'agata C, Ambrosini R, et al. A simple model to evaluate ice melt over the ablation area of glaciers in the Central Karakoram National Park, Pakistan. Annals of Glaciology. 2015; 56(70):202–216.

28. Pratap B, Dobhal D, Mehta M, Bhambri R. Influence of debris cover and altitude on glacier surface melting: a case study on Dokriani Glacier, central Himalaya, India. Annals of Glaciology. 2015; 56(70):9–16.
29. Baldasso V, Soncini A, Azzoni R, Diolaiuti G, Smiraglia C, Bocchiola D. Recent evolution of glaciers in Western Asia in response to global warming: the case study of Mount Ararat, Turkey. Theoretical and Applied Climatology. 2018; p. 1–15.